All-reflective Michelson, Sagnac, and Fabry–Perot interferometers based on grating beam splitters

Ke-Xun Sun

TWS Technologies, Inc., 632 Des Moines Place, San Jose, California 95133

Robert L. Byer

Edward L. Ginzton Laboratory, Stanford University, Stanford, California 94305-4085

Received December 3, 1997

All-reflective Michelson, Sagnac, and Fabry–Perot interferometers based on grating beam splitters are experimentally demonstrated at a wavelength of 1064 nm. A 1200-groove/mm grating diffracting 0 and −1 orders with an efficiency of 48.2% for each order was used as a near-50/50 beam splitter. The all-reflective Sagnac and Michelson interferometers were formed by reintroducing both of the diffracted beams back to the grating. The Fabry–Perot interferometer was formed in a Littrow configuration by using a 1700-groove/mm grating with a blazing efficiency of 91% as a cavity coupler. These interferometers encompass all the fundamental configurations of all-reflective laser interferometric gravitational-wave detectors, promising improved wave-front quality by avoiding volume thermal effects in transmissive optics under high-power laser illumination.

OCIS codes: 050.1950, 120.3180, 230.1360.

The foundation for Michelson, Sagnac, and Fabry–Perot interferometry is the coherent addition of correlated optical waves, traditionally achieved by splitting and recombining a single optical beam with a transmissive beam splitter.[1,2] However, high optical power or extreme wavelengths pose problems to transmissive optics. In the proposed advanced Laser Interferometric Gravitational-wave Observatory interferometer[3] (LIGO) the central beam splitter is to be illuminated with more than 10 kW of laser power at 1064 nm.[3] Such high power may lead to thermal lensing and birefringence in the beam splitter and arm optics, resulting in a lowered contrast ratio of the interference fringe.[4,5] The Sagnac interferometer could alleviate these problems by counterpropagating two laser beams through a common optical path.[2] Eliminating transmissive optics altogether through use of reflective beam splitters can substantially reduce the magnitude of volume thermal distortions. Use of diffractive optics for this purpose has been discussed by Byer[6] and Drever.[7] In addition, the all-reflective interferometer topology permits the use of opaque or less transmissive substrates such as silicon and sapphire, which have better thermal properties and lower thermal noise[8] than fused silica. We report the experimental demonstration of all-reflective, grating-beam-splitter-based interferometers, particularly those of interest to gravitational-wave detection: Michelson, Sagnac, and Fabry–Perot interferometers.

A reflective grating is a wave-front segmenting and diffracting device. For a laser beam of wavelength λ incident onto the grating, the output angle θ_m of the mth diffraction order is given by the grating equation[1]

$$d(\sin\theta_m - \sin\theta_{\mathrm{inc}}) = m\lambda\,, \tag{1}$$

where θ_{inc} is the incident angle and d is the grating period. A grating may produce multiple diffraction orders. An interferometer is formed when these diffraction orders are retroreflected back onto the grating, then rediffract, and interfere. To replace a transmissive beam splitter with a reflective grating beam splitter, the $m = 0$ and $m = -1$ diffraction orders should be in the directions convenient to the interferometer geometry, whereas the other diffraction orders should be eliminated to reduce energy loss. This requirement can be met by properly choosing the incident angle θ_{inc} and the grating period d. For example, for the angle between the 0 and −1 orders to be 90°, Eq. (1) requires that

$$\sqrt{2}\,d\,\sin(\theta_{\mathrm{inc}} + 45^\circ) = \lambda\,, \tag{2}$$

which in turn requires that $1 < \lambda/d \leq \sqrt{2}$, simultaneously eliminating the other diffraction orders. The energy distribution among diffraction orders depends on the polarization, incident angle, and wavelength of the incident beam and on the grating parameters, such as shape and density of the grooves and material properties of the grating surface.[9] The relative phase of each diffraction order can either be determined from a scattering matrix formalism[10] or directly calculated from the boundary conditions.

In proof-of-principle experiments for Michelson and Sagnac interferometers we used a 1200-groove/mm holographic metal grating as the beam splitter and a 26-mW, 1064-nm diode-pumped Nd:YAG laser. The polarization plane of the incident laser beam was parallel to the grating grooves and perpendicular to the plane of incidence. At $\theta_{\mathrm{inc}} \approx 32.5^\circ$, 48.2% of the input power was measured in both the 0 and the −1 orders. The scattering, ghost, and absorption losses accounted for the 3.6% loss in total diffracted power. The angle between the original 0 and −1 diffraction orders was 80.1°.

Figure 1(a) shows the experimental setup for the all-reflective Michelson grating interferometer. The 0 order, with a diffraction angle of $\theta_0 = \theta_{\mathrm{inc}} \approx 32.5^\circ$

0146-9592/98/080567-03$15.00/0

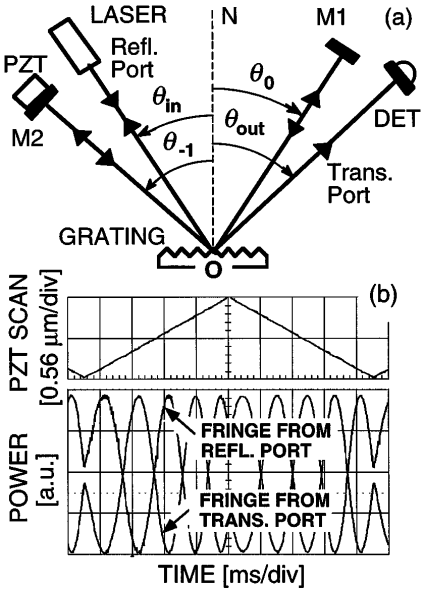

Fig. 1. (a) Experimental setup for the all-reflective Michelson interferometer based on a grating beam splitter: LASER, 1064 nm diode-pumped Nd:YAG laser; other abbreviations defined in text. (b) Waveforms from the all-reflective Michelson interferometer. Upper trace: PZT scan; each ramp is over a full wavelength. Sinusoidal traces: fringes from the reflecting and transmitting ports. The traces are at the same power scale.

on the opposite side of the grating normal, N, from the incident beam, was sent to mirror M1. The -1 order, with a diffraction angle $\theta_{-1} \approx -47.6°$ to the same side of the grating normal as the incident beam, was sent to mirror M2. These beams were retroreflected from M1 and M2 onto the grating again, and new diffraction orders were produced. The new -1 order of the reflected beam from M1 and the new 0 order of the reflected beam from M2 diffracted into a common direction of 47.6° to the right of the grating normal to form the transmitting-port (Trans. Port) fringe, which was sensed by a detector (DET). Similarly, the new 0 order of the reflected beam from M1 and the new -1 order of the reflected beam from M2 diffracted into a common direction of 32.5° to the left of the grating norm, reflecting backward to the laser to form a reflecting port (Refl. Port) fringe. A small fraction of this reflected beam from a beam splitter in the input beam path [not shown in Fig. 1(a)] was detected to record the reflecting port fringe. M2 was attached to a piezoelectric transducer (PZT) to scan the arm length.

Figure 1(b) shows the outputs from the all-reflective Michelson interferometer's transmitting and reflecting ports when M2 was scanned over a distance greater than a full wavelength. Interference fringes were observed at both ports. The sinusoidal outputs were 180° out of phase with the oscilloscope reading precision of ±2°, indicating the π-phase difference between the output waves from the transmitting and reflecting ports. The minimum power at the transmitting port and the maximum power at the reflecting port were 0.11 and 25.7 mW, respectively, giving a contrast ratio of ~0.99.

Figure 2(a) shows the experimental setup for the all-reflective zero-area Sagnac interferometer, where a loop connecting the original 0 and -1 diffraction orders was made through high reflectors M1, M3, and M2. This arrangement is an all-reflective version of the Sagnac interferometer experiment based on transmissive optics described in Ref. 2.

Figure 2(b) shows the outputs from the transmitting and reflecting ports of the all-reflective Sagnac interferometer for the same M2 scan as before. The dark fringe is formed at the transmitting port and the bright fringe is formed at the reflecting port, just as in a Sagnac interferometer with a transmissive beam splitter. In fact, the output from the transmitting port of the Sagnac interferometer is approximately proportional to $\sum_n J_n^2(m_d)\sin^2(n\pi f/2f_{\max})$, where J_n is the nth-order Bessel function, m_d is the phase modulation index that is due to the mirror displacement, f is the frequency of the mirror movement, and $f_{\max}$ is the frequency for maximum response of the first sideband.[2] Because of the short arm length (108 mm for OM_1), $f_{\max} = 2.78$ GHz, and hence the near-dc mirror movement at $f = 110$ Hz did not affect the dark fringe at the transmitting port and the bright fringe at the reflecting port appreciably. The larger beam spot size (~3.5 mm) in the Sagnac interferometer compared with that (~2.8 mm) in the Michelson interferometer led to a lowered contrast ratio (0.93) owing to grating nonuniformity.

Figure 3(a) shows the experimental setup of the all-reflective Fabry–Perot grating cavity, where the grating is mounted in a Littrow configuration.

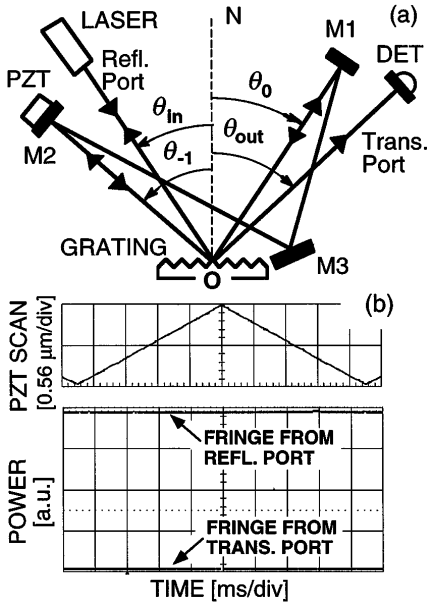

Fig. 2. (a) Experimental setup for the all-reflective zero-area Sagnac interferometer based on a grating beam splitter. Abbreviations are the same as in Fig. 1(a). M3, additional mirror to form the Sagnac loop. (b) Waveforms from the all-reflective Sagnac interferometer. Upper trace: PZT scan; each ramp is over a full wavelength. Middle trace: output from the reflecting port. Lower trace: output from the transmitting port.

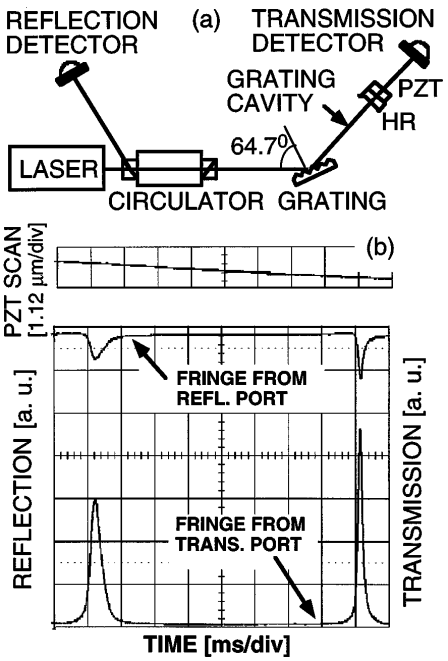

Fig. 3. (a) Experimental setup for the Fabry–Perot grating cavity: HR, high reflector; CIRCULATOR, Faraday isolator. (b) Waveforms from the all-reflective Fabry–Perot cavity. PZT scan; each ramp is over a half wavelength. Middle trace: output from the reflecting port. Lower trace: output from the transmitting port.

The grating was a 1700-groove/mm metal grating with a 91% diffraction efficiency at blazing angle 64.7°. The cavity length was 20 mm. Transmission and reflection from the grating cavity were observed from the back port of the circulator and from a small leakage (0.1%) from the high reflector, respectively. This conventional Littrow configuration is simpler than using a weak grating as a cavity coupler as suggested in Ref. 6 and 7, which results in an extra output port and added complexity.

Figure 3(b) shows the transmission and reflection interference fringes, which exhibit a cavity finesse of 53. The broadening of the resonance at the higher voltage of the PZT scan was due to PZT tilting and caused mix-in of higher-order transverse modes. A higher-power laser was used to raise the intracavity power density to 1.57 W/mm^2 at the resonance peak, and no appreciable change in the interference fringe was observed at such a power density level approaching that of the initial Laser Interferometric Gravitational-wave Observatory.

Several practical issues that may occur when one is using grating beam splitters in large-scale interferometers can be solved with existing technology. First, because of its dispersion, the grating beam splitter requires that laser center frequency drift Δf be smaller than that restricted by maximum allowable angular deviation $\Delta\theta_m$ from the designated direction, $\Delta f \leq (c/\lambda^2)|d\cos(\theta_m)/m|\Delta\theta_m$. For an angular pointing accuracy of $\Delta\theta_{-1} = 10^{-7}$ rad, as needed in a kilometer-scale interferometer, $\Delta f \leq 21$ MHz for $\theta_{-1} = -30°$. Frequency stability of this order has been demonstrated for an I_2-stabilized Nd:YAG laser, where long-term stability of $1{:}10^{13}$ or ~30 Hz is possible.[11]

Second, metal gratings cannot handle a laser beam of an average power of kilowatts. However, gratings that are etched on the top of multilayer dielectric coatings[12] have lower loss, higher damage threshold, and more precisely controllable diffraction characteristics than traditional metal gratings and are expected to fulfill the requirements of interferometers in gravitational-wave detection. The absorption loss in dielectric coatings is currently achievable down to 10^{-6}–10^{-5}, significantly lower than volume absorption of $\sim 10^{-4}$ in transmissive optics. The effect of grating shape change on the interferometer contrast ratio is estimated to be minimal compared with that of volume transmissive optics under same high-power laser illumination.

In summary, we have experimentally demonstrated grating-beam-splitter-based, all-reflective Michelson, Sagnac, and Fabry–Perot interferometers, which include the interferometric configurations needed for building an all-reflective, advanced Laser Interferometric Gravitational-wave Observatory interferometer. Further, the diffraction grating's multiport capability permits new diffractive interferometer architectures that have advantages over two-port topologies.[10]

This research was partially supported by the National Science Foundation (grant NSF PHY 92-15157) and by funds from TWS Technologies, Inc., and R. L. Byer. We thank G. Y. Yin for loan of the gratings.

References

1. M. Born and E. Wolf, *Principles of Optics,* 6th ed. (Pergamon, Oxford, 1987).
2. K.-X. Sun, M. M. Fejer, E. Gustafson, and R. L. Byer, Phys. Rev. Lett. **76,** 3053 (1996).
3. For example, see, A. Abramovici, W. E. Althouse, R. W. P. Drever, Y. Gursel, S. Kawamura, F. Raab, D. Shoemaker, L. Sievers, R. E. Spero, K. S. Thorne, R. E. Vogt, R. Weiss, S. Whitcomb, and M. E. Zucker, Science **256,** 5055 (1992).
4. W. Winkler, K. Danzmann, A. Rudiger, and R. Schilling, Phys. Rev. A **44,** 7022 (1991).
5. W. Winkler, A. Rudiger, R. Shilling, K. A. Strain, and K. Danzmann, Opt. Commun. **112,** 245 (1994).
6. R. L. Byer, in *Gravitational Astronomy: Instrument Design and Astrophysical Prospects,* D. E. McClelland and H.-A. Bachor, eds. (World Scientific, Singapore, 1990).
7. R. Drever, in *Proceedings of the Seventh Marcel Grossman Meeting on General Relativity,* M. Keiser and R. T. Jantzen, eds. (World Scientific, Singapore, 1995).
8. P. Saulson, Phys. Rev. D **42,** 2437 (1990).
9. R. Petit, ed. *Electromagnetic Theory of Gratings* (Springer-Verlag, Berlin, 1980).
10. K.-X. Sun, presented at the Optical Society of America 1997 Annual Meeting, Long Beach, Calif., October 11–17, 1997.
11. A. Arie and R. L. Byer, Appl. Opt. **32,** 7382 (1993).
12. M. Perry, R. Boyd, J. Britten, D. Decker, B. Shore, C. Shannon, and E. Shults, Opt. Lett. **20,** 940 (1995).